PERIODICA POLYTECHNICA SER. MECH. ENG. VOL. 48, NO. 2, PP. 151–161 (2004)

COMPARISON OF SOME DATA REDUCTION SCHEMES FOR COMPOSITE DELAMINATION SPECIMENS

András SZEKRÉNYES

Department of Applied Mechanics
Budapest University of Technology and Economics
H–1521 Budapest, PoB 11, Hungary
Phone: +36 1 463 1170, Fax: +36 1 463 3471
e-mail: szeki@mm.bme.hu

Received: June 30, 2004

Abstract

Three different solutions for orthotropic, beam-like fracture specimens were compared in the current work. A beam theory-based approach was developed previously by the author. Another solution based on refined plate theory was also considered. Finally, equations based on a numerical calibration technique were utilized as a third solution. These solutions were extended for the case of composite double-cantilever beam, end-loaded split and single-cantilever beam fracture specimens. All the three solutions give reliable expressions for the double-cantilever beam. In contrast for the end-loaded split and the single-cantilever beam coupons the three models give quite distinct results, especially for the mode ratio of the single-cantilever beam specimen.

Keywords: beam theory, strain energy release rate, mode ratio, delamination.

1. Introduction

The interlaminar fracture is the primary failure mode in laminated composite structures. The interlaminar fracture toughness (known as the resistance to delamination) is determined through beam-like specimens. The double-cantilever beam (DCB) specimen is a standard tool for measuring the mode-I toughness. For this coupon numerous improved beam theory-based solutions were developed in the literature, which incorporates the Winkler foundation and Timoshenko beam theory [1, 2, 3]. For mode-II specimens beam theory [4,5] and the finite element method [6] was applied to obtain refined solutions for the strain energy release rate. The solution by Wang and Qiao [7] for the end-notched flexure (ENF) the specimen should be mentioned due to its elegance and simplicity. For mixed-mode I/II testing many configurations were developed by the researchers, see for instance [8, 9, 10]. The standard mixed-mode bending (MMB) is the most universal method, which is intensively applied nowadays [11, 12]. The MMB specimen has several disadvantages, especially that it requires a complex fixture. The role of material orthotropy on the fracture toughness of certain composite specimens was investigated by BAO et al. [13]. In their work closed-form equations were derived based on numerical calculations for the DCB, the mode-II end-loaded split (ELS) and the mixed-mode

single-cantilever beam (SCB) specimens. Under mixed-mode I/II condition the mode decomposition is an important issue. Different methods were developed by the researchers to solve this problem. The beam theory-based global method was developed by WILLIAMS [14], while the local method was established by SUO and HUTCHINSON [15, 16]. The crack tip element analysis is a third analytical method [17, 18], which is equivalent to the local approach. In the work of BRUNO and GRECO a refined plate model including shear effect was applied, the individual mode components were evaluated by using the interlaminar stresses and displacements [19, 20]. This method was found to give the same result as Williams' global approach. The global method was improved by the effect of Winkler foundation and transverse shear in [21]. The local method was completed with shear effect by WANG and QIAO [22]. Finally, the virtual crack-closure technique (VCCT) should be mentioned, which is widely applied for mode decomposition and energy release rate calculation [23].

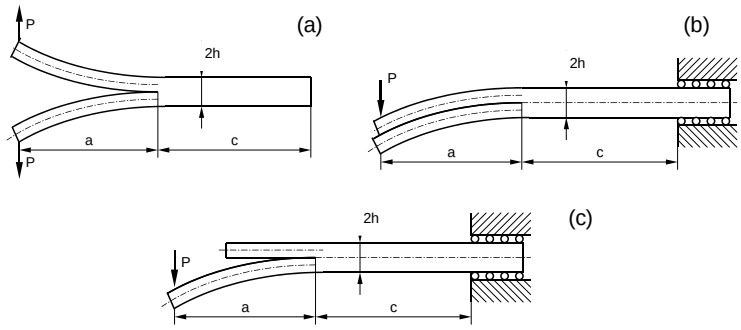

Fig. 1. DCB (a), ELS (b) ans SCB (c) delamination specimens

In the current work the DCB, ELS and SCB specimens are examined. Three different solutions are extended for these fracture specimens including mode-mixity: beam theory-based solution [7, 21], solution based on refined plate theory [19, 20] and a numerical solution by BAO et al. [13]. Furthermore, the mode decomposition based on the VCCT [23] was achieved in the case of the mixed-mode I/II SCB coupon. The delamination specimens are illustrated in *Fig. 1*.

2. Beam Theory-Based Solution

Based on previous works [7, 14, 21], the following formulae may be derived for the individual energy release rate components of composite specimens under general

mixed-mode I/II loading conditions:

$$G_I = \frac{M_I^2(12 + f_{W2} + f_{T2})}{b^2h^3E_{11}}, \tag{1}$$

$$G_{II} = \frac{M_{II}^2(9 + f_{SH2})}{b^2h^3E_{11}}, \tag{2}$$

where the coefficients in *Eqs.* (1) and (2) are:

$$f_{W2} = 6.64\left(\frac{h}{a}\right)\left(\frac{E_{11}}{E_{33}}\right)^{\frac{1}{4}}\eta_1 + 3.68\left(\frac{h}{a}\right)^2\left(\frac{E_{11}}{E_{33}}\right)^{\frac{1}{2}}\eta_2, \tag{3}$$

$$f_{SH2} = 1.96\left(\frac{h}{a}\right)\left(\frac{E_{11}}{G_{13}}\right)^{\frac{1}{2}} + 0.43\left(\frac{h}{a}\right)^2\left(\frac{E_{11}}{G_{13}}\right), \tag{4}$$

$$f_{T2} = \frac{1}{k}\frac{E_{11}}{G_{13}}\left(\frac{h}{a}\right)^2. \tag{5}$$

The mode-I and mode-II bending moments may be obtained as follows [14]:

$$M_I = (M_1 - M_2)/2, \qquad M_{II} = (M_1 + M_2)/2, \tag{6}$$

where M_1 and M_2 are reduced bending moments at the crack tip. The subscript refers to the upper (1) and lower (2) specimen arm. The coefficients in *Eq.* (3) are defined as:

$$\begin{aligned} &\eta_1 = 2\sqrt{2},\ \eta_2 = 2 \qquad &&\text{if: } M_1 = -M_2, \\ &\eta_1 = \eta_2 = 1, &&\text{otherwise.} \end{aligned} \tag{7}$$

In the case of the DCB specimen (see *Fig. 1a*) the bending moments at the crack tip are $M_1 = -Pa$, $M_2 = Pa$. Thus the fracture energy from *Eq.* (1) considering *Eq.* (7) becomes:

$$G_I^{\text{DCB}} = \frac{12P^2a^2}{b^2h^3E_{11}}\left[1 + 1.57\left(\frac{h}{a}\right)\left(\frac{E_{11}}{E_{33}}\right)^{\frac{1}{4}} + 0.61\left(\frac{h}{a}\right)^2\left(\frac{E_{11}}{E_{33}}\right)^{\frac{1}{2}} + 0.1\left(\frac{h}{a}\right)^2\left(\frac{E_{11}}{G_{13}}\right)\right]. \tag{8}$$

Let us consider the case of the mode-II ELS coupon in *Fig. 1b*, whereas: $M_1 = M_2 = Pa$, from *Eq.* (2) we obtain:

$$G_{II}^{\text{ELS}} = \frac{9P^2a^2}{4b^2h^3E_{11}}\left[1 + 0.22\left(\frac{h}{a}\right)\left(\frac{E_{11}}{G_{13}}\right)^{\frac{1}{2}} + 0.048\left(\frac{h}{a}\right)^2\left(\frac{E_{11}}{G_{13}}\right)\right]. \tag{9}$$

For the SCB specimen we can write: $M_1 = 0$, $M_2 = Pa$ based in *Fig. 1c*, thus we obtain the components from *Eqs.* (1) and (2):

$$G_I^{\mathrm{SCB}} = \frac{12P^2a^2}{4b^2h^3E_{11}}\left[1 + 0.55\left(\frac{h}{a}\right)\left(\frac{E_{11}}{E_{33}}\right)^{\frac{1}{4}} + 0.31\left(\frac{h}{a}\right)^2\left(\frac{E_{11}}{E_{33}}\right)^{\frac{1}{2}} + 0.1\left(\frac{h}{a}\right)^2\left(\frac{E_{11}}{G_{13}}\right)\right], \tag{10}$$

$$G_{II}^{\mathrm{SCB}} = \frac{9P^2a^2}{4b^2h^3E_{11}}\left[1 + 0.22\left(\frac{h}{a}\right)\left(\frac{E_{11}}{G_{13}}\right)^{\frac{1}{2}} + 0.048\left(\frac{h}{a}\right)^2\left(\frac{E_{11}}{G_{13}}\right)\right]. \tag{11}$$

The mode ratio (G_I/G_{II}) of the SCB specimen can be obtained by combining *Eqs.* (10)-(11). Note that *Eq.* (9) is equivalent to *Eq.* (11), i.e. the mode-II component for the SCB is the same as for the ELS coupon.

3. Solution Based on Numerical Calibration

BAO et al. [13] derived the following expressions for the DCB specimen based on finite element calculations:

$$G_I^{\mathrm{DCB}} = \frac{12P^2a^2}{b^2h^3E_{11}}\left[1 + (0.677 + 0.146\beta - 0.0178\beta^2 + 0.00242\beta^3)\lambda^{-\frac{1}{4}}\left(\frac{h}{2}\right)\right]^2. \tag{12}$$

The same manner was used to obtain the expressions below for the SCB specimen:

$$G_I^{\mathrm{SCB}} = \frac{12P^2a^2}{4b^2h^3E_{11}}\left[1 + (0.677 + 0.146\beta - 0.0178\beta^2 + 0.00242\beta^3)\lambda^{-\frac{1}{4}}\left(\frac{h}{2}\right)\right]^2, \tag{13}$$

$$G_{II}^{\mathrm{SCB}} = G_{II}^{ELS} = \frac{9P^2a^2}{4b^2h^3E_{11}}\left[1 + (0.206 + 0.0761\beta - 0.00978\beta^2 + 0.00112\beta^3)\lambda^{-\frac{1}{4}}\left(\frac{h}{2}\right)\right]^2. \tag{14}$$

where:

$$\lambda = \frac{E_{33}}{E_{11}}, \qquad \beta = \frac{(E_{11}E_{33})^{\frac{1}{2}}}{G_{13}} - \nu_{13}\nu_{31} - 1. \tag{15}$$

Note that for the ELS specimen *Eq.* (13) can be used.

4. Solution Based on a Refined Plate Model

BRUNO and GRECO [19, 20] utilized a linear elastic interface model between two Reissner-Mindlin plates. Their solution can be extended for the DCB and SCB coupons. The solutions after some transformation can be written as:

$$G_I^{\mathrm{DCB}} = \frac{12P^2a^2}{b^2h^3E_{11}}\left[1 + 0.63\left(\frac{h}{a}\right)\left(\frac{E_{11}}{G_{13}}\right)^{\frac{1}{2}} + 0.1\left(\frac{h}{a}\right)^2\left(\frac{E_{11}}{G_{13}}\right)\right], \tag{16}$$

$$G_I^{\mathrm{SCB}} = \frac{12P^2a^2}{4b^2h^3E_{11}}\left[1 + 0.63\left(\frac{h}{a}\right)\left(\frac{E_{11}}{G_{13}}\right)^{\frac{1}{2}} + 0.1\left(\frac{h}{a}\right)^2\left(\frac{E_{11}}{G_{13}}\right)\right], \tag{17}$$

$$G_{II}^{\mathrm{SCB}} = G_{II}^{\mathrm{ELS}} = \frac{9P^2a^2}{4b^2h^3E_{11}}. \tag{18}$$

For the ELS specimen *Eq.* (18) applies. It should be noted that this formulation gives equivalent result to the simple beam theory with respect to the mode-II component, as it can be seen from *Eq.* (18).

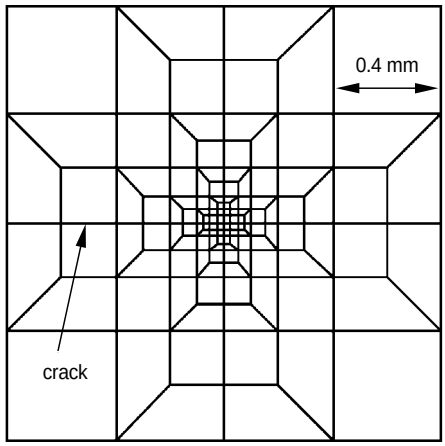

Fig. 2. FE mesh around the crack tip

5. Mode Decomposition Using the VCCT Method

For the mixed-mode SCB specimen a series of FE models were constructed to obtain mode ratios for the SCB specimen in the crack length range of $a = 20 - 100$ mm. The models were developed in the commercial code COSMOS/M 2.0 using PLANE2D elements under plane stress state, which is consistent with beam

formulation of the problem. The specimens were 150 mm long, 20 mm wide and $2h = 6.1$ mm thick. The material properties were given for glass/polyester composite specimens manufactured in our laboratory. The flexural moduli of the specimens were determined through a non-standard three-point bending test, which resulted in $E_{11} = 33$ GPa. Further material properties were predicted by using Niederstadt's [24] approximate rule of mixture: $E_{33} = 7.2$ GPa, $G_{13} = 3$ GPa and $\nu_{13} = \nu_{31} = 0.27$. According to the VCCT method the energy release rate components are:

$$G_I = \frac{1}{2b\Delta a} F_y(v_1 - v_2), \tag{19}$$

$$G_{II} = \frac{1}{2b\Delta a} F_x(u_1 - u_2), \tag{20}$$

where F_x, F_y are nodal forces at the crack tip, v_1, v_2, u_1, u_2 are nodal displacements from Δa distance to the crack tip and b is the specimen width. A finite element mesh around the crack tip, suggested by DAVIDSON et al. [9] was applied, as it is shown in *Fig. 2*. Crack tip elements with $\Delta a = 0.025$ mm were used (*Fig. 2*). At each crack length the specimens were loaded by $P = 1$ N at the end and only the mode-mixity was determined.

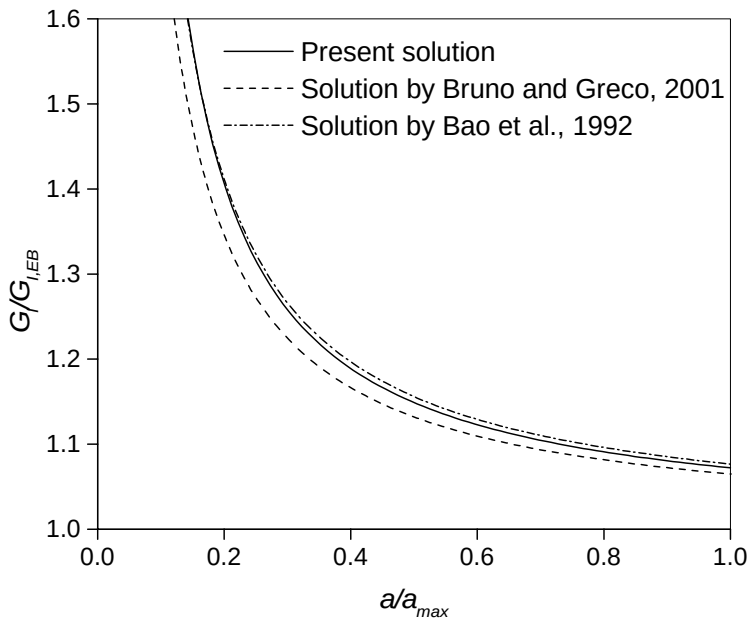

Fig. 3.

6. Results

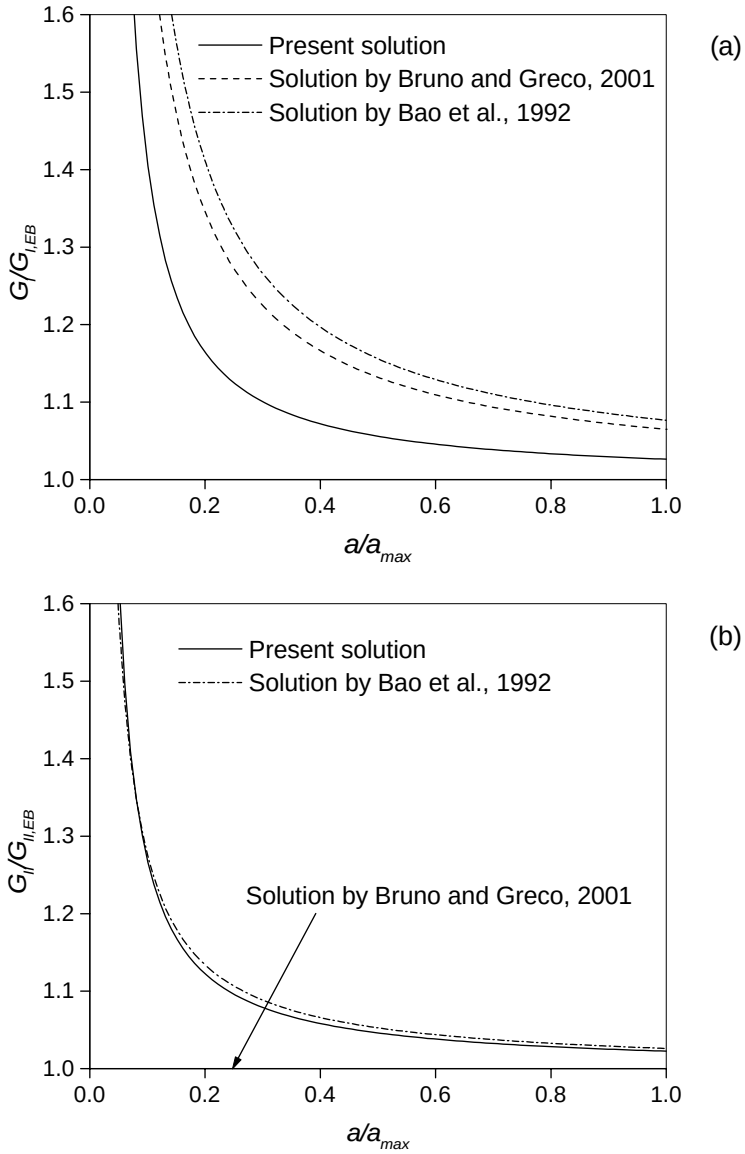

Fig. 4.

All the equations were normalized with the results of Euler-Bernoulli beam theory. These are the first terms in *Eqs.* (8)-(11). The normalized strain energy

release rates are plotted against the normalized crack length, $a/a_{\max}$, where $a_{\max} = 100$ mm.

For the DCB specimen the three different solutions are plotted in *Fig. 3*. In this respect Bao's solution seems to be the best. Although our solution is somewhat closer to the former one as the solution by Bruno and Greco, the difference between them is not notable. As a consequence all the three solutions are in good agreement in this case.

The results for the mixed-mode I/II SCB specimen are illustrated in *Figs. 4a* and *b*. In the case of the mode-I component (*Fig. 4a*) some differences can be seen, especially between our and Bao's solution. The plate model by Bruno and Greco gives the curve between the former two solutions. The normalized mode-II component is presented in *Fig. 4b*. The agreement was excellent between our model and the one by Bao et al. In contrast the mode-II component is equivalent to the formula of Euler-Bernoulli beam model in accordance with the formulation of Bruno and Greco.

In the case of the mode-II ELS specimen the same results were obtained as illustrated in *Fig. 4b*.

Table 1. Mode ratios (G_I/G_{II}) by different methods, SCB specimen

a* [mm]	20	30	40	50	60	70	80	90	100
	1.353	1.346	1.343	1.341	1.339	1.339	1.338	1.337	1.337*
	1.794	1.633	1.555	1.509	1.479	1.458	1.442	1.430	1.420**
	1.659	1.551	1.497	1.464	1.442	1.427	1.415	1.406	1.399***
	1.250	1.176	1.144	1.120	1.105	1.093	1.085	1.078	1.073****

* present solution, ** solution by Bruno and Greco, 2001, ***solution by Bao et al., 1992, ****VCCT method

The mode ratios by four different approximations are listed in *Table 1*. Quite distinct results were obtained even in this case. The model by Bruno and Greco shows large mode-I dominance. Bao's numerical formulation gives similar values, however, these are slightly less than those calculated from the model by Bruno and Greco. Our beam theory-based approach predicts approximately constant mode ratios, which is equivalent to the result of Williams' classical formulation [14]. Finally the plane stress FE model also shows notable crack length dependence of the mode ratio. The mode-I dominance is not as significant here as in the case of Bao's and Bruno and Greco's solution. The summary of the results indicates that the mode ratio depends on the method applied for data reduction. Values for the mode ratio were obtained within 1.8 to 1.25 at $a = 20$ mm and 1.4 to 1 at $a = 100$ mm by four different methods and with hyperbolic decay as the crack length increases. Except for our solution the three other methods show notable crack length dependence.

7. Discussion

As a consequence under pure mode-I and mode-II conditions it seems that our solution closely agrees with Bao's numerical model. In contrast under mixed-mode I/II case some discrepancies were observed, which should be clarified.

According to our formulation the total strain energy release rate was obtained by a superposition scheme, which incorporates the effect of Winkler-foundation, transverse shear and crack tip deformation. Interaction between them was neglected. Note that Steiner's theorem was considered in the case of the elastic foundation.

Bao's numerical model provides the larger improvements. In that work the SCB specimen was treated as the superposition of the pure mode-I DCB and the pure mode-II ELS specimens. In our previous work [21] it was shown that due to Steiner's theorem the elastic foundation behaves differently under mode-I than under mixed-mode I/II loading condition. Consequently, this effect was ignored in Bao's equations.

The refined plate model by Bruno and Greco affirms the significance of bending–shear interaction. Their model does not provide improved solution for the mode-II component, whereas our and Bao's solution show that the mode-II component should be contributed apart from the simple beam theory.

It should be kept in mind that in the case of the VCCT method the convergence and accuracy of the solution is not guaranteed due to the singularity nature of the problem. The results are sensitive to the size and number of finite elements around the crack tip zone. Furthermore the mesh refinement around the crack tip involves the increase in the mode-II component.

The problem is that the mode-mixity is difficult to be determined experimentally. It is possible only in some special cases. Such a case is the mixed-mode bending (MMB) specimen. DUCEPT et al. [23] applied an experimental mode decomposition technique, which provided similar results as our beam theory-based formulation. Since this is the only source for experimental mode decomposition all the models presented here should be applied with caution with respect to the mode ratio. On the other hand the total strain energy release rate of the mixed-mode SCB specimen is predicted with similar accuracy by the three different solutions.

8. Conclusions

A comparative study was performed using three different solutions for common delamination specimens, such as the mode-I DCB, the mode-II ELS and the mixed-mode I/II SCB specimen. Furthermore the mode ratio was evaluated by the VCCT method too. Although only the DCB specimen is accepted as a standard tool, the presented results here would be similar for other types of delamination coupons too.

The comparison of the results shows somewhat different consequences. If only pure mode-I or mode-II condition is investigated our and Bao's solution closely

agrees. In the model by Bruno and Greco the mode-II component suffers from any improvements apart from simple beam theory. The most conspicuous discrepancies were experienced in the case of the mixed-mode SCB specimen. Neither the mode-I component nor the mode ratio agrees if we compare the results from three different closed-form solutions. Neither the VCCT method gives mode ratio values close to any of the mentioned solutions. As a consequence the mode ratio depends on the technique applied. Apart from this another problem is that the mode ratio can not be determined experimentally.

Acknowledgement

This research work was supported by the fund OTKA T037324. The authors are grateful to Tonny Nyman for providing the reference by WILLIAMS [14]. We wish to thank Barry D. Davidson for sending his work [9] to us.

References

[1] OLSSON, R., A Simplified Improved Beam Analysis of the DCB Specimen, *Composites Science and Technology*, **43** (1992), pp. 329–338.

[2] OZDIL, F. – CARLSSON, L. A. – DAVIES, P., Beam Analysis of Angle-Ply Laminate End-Notched Flexure Specimens, *Composites Science and Technology*, **58** (1998), pp. 1929–1938.

[3] WILLIAMS, J. G., End Corrections for Orthotropic DCB Specimens, *Composites Science and Technology*, **35** (1998), pp. 367–376.

[4] OZDIL, F. – CARLSSON, L. A. – DAVIES, P., Beam Analysis of Angle-Ply Laminate End-Notched Flexure Specimens, *Composites Science and Technology*, **58** (1998), pp. 1929–1938.

[5] CARLSSON, L. A. – GILLESPIE, J. W. – PIPES, R. B., On the Analysis and Design of the End Notched Flexure (ENF) Specimen for Mode II Testing, *Journal of Composite Materials*, **20** (1986), pp. 594–604.

[6] WANG, Y. – WILLIAMS, J. G., Corrections for Mode II Fracture toughness Specimens of Composite Materials, *Composites Science and Technology*, **43** (1992), pp. 251–256.

[7] WANG, J. – QIAO, P., Novel Beam Analysis of the End Notched Flexure Specimen for Mode-II Fracture, *Engineering Fracture Mechanics*, **71** (2004), pp. 219–231.

[8] LAI, Y.–H. – RAKESTRAW, M. D. – DILLARD, D. A., The Cracked Lap Shear Specimen Revisited – a Closed Form Solution, *International Journal of Solids and Structures*, **33** (1996), pp. 1725–1743.

[9] DAVIDSON, B. D. – SUNDARARAMAN, V., A Single Leg Bending Test for Interfacial Fracture Toughness Determination, *International Journal of Fracture*, **78** (1996), pp. 193–210.

[10] TRACY, G. D. – FERABOLI, P. – KEDWARD, K. T., A New Mixed Mode Test for Carbon/Epoxy Composite Systems, Composites Part A: *Applied Science and Manufacturing*, **34** (2003), pp. 1125–1131.

[11] REEDER, J. R. – CREWS, J. R., Mixed-Mode Bending Method for Delamination Testing, *AIAA Journal* **28** (1990), pp. 1270–1276.

[12] KIM, B. W. – MAYER, A. H., Influence of Fiber Direction and Mixed-Mode Ratio on Delamination Fracture Toughness of Carbon/Epoxy Laminates, *Composites Science and Technology*, **63** (2003), pp. 695–713.

[13] BAO, G. – HO, S. – SUO, Z. – FAN, B., The Role of Material Orthotropy in Fracture Specimens for Composites, *International Journal of Solids and Structures*, **29** (1992), pp. 1105–1116.

[14] WILLIAMS, J. G., On the Calculation of Energy Release Rates for Cracked Laminates, *International Journal of Fracture*, **36** (1988), pp. 101–119.
[15] SUO, Z., Delamination Specimens for Orthotropic Materials, *Journal of Applied Mechanics*, **57** (1990), pp. 627–634.
[16] SUO, Z. – HUTCHINSON, J. W., Interface Crack between Two Elastic Layers, *International Journal of Fracture*, **43** (1990), pp. 1–18.
[17] SUNDARARAMAN, V. – DAVIDSON, B. D., An Unsymmetric End-Notched Flexure Test for Interfacial Fracture Toughness Determination, *Engineering Fracture Mechanics*, **60** (1998), pp. 361–377.
[18] SUNDARARAMAN, V. – DAVIDSON, B. D., An Unsymmetric Double Cantilever Beam Test for Interfacial Fracture Toughness Determination, *International Journal of Solids and Structures* **34** (1997), pp. 799–817.
[19] BRUNO, D. – GRECO, F., Mixed Mode Delamination in Plates: a Refined Approach, *International Journal of Solids and Structures*, **38** (2001), pp. 9149–9177.
[20] BRUNO, D. – GRECO, F., Delamination in Composite Plates: Influence of Shear Deformability on Interfacial Debonding, *Cement & Concrete Composites*, **23** (2001), pp. 33–45.
[21] SZEKRÉNYES, A. – UJ, J., Beam and Finite Element Analysis of Quasi-Unidirectional SLB and ELS Specimens, *Composites Science and Technology*, **64** (2004), pp. 2393–2406.
[22] WANG, J. – QIAO, P., Interface Crack between Two Shear Deformable Elastic Layers, *Journal of the Mechanics and Physics of Solids*, **52** (2004), pp. 891–905.
[23] DUCEPT, F. – GAMBY, D. – DAVIES, P., A Mixed-Mode Failure Criterion Derived from Tests of Symmertic and Asymmetric Specimens, *Composites Science and Technology*, **59** (1999), pp. 609–619.
[24] THAMM, F., Strength of Plastic Materials II. Budapest 1985 (in Hungarian).